International Journal of Biological Macromolecules 280 (2024) 136019

Contents lists available at ScienceDirect

International Journal of Biological Macromolecules

journal homepage: www.elsevier.com/locate/ijbiomac

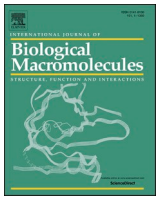

Research Paper

Bovine serum albumin and lysozyme nanofibers as versatile platforms for preserving loaded bioactive compounds

Rocío Díaz-Puertas [a], Enrique Rodríguez-Cañas [a], María Jesús Lozoya-Agulló [a], Pedro Valentín Badía-Hernández [a], Francisco Javier Álvarez-Martínez [a], Alberto Falcó [b,*], Ricardo Mallavia [a,*]

[a] Instituto de Investigación, Desarrollo e Innovación en Biotecnología Sanitaria de Elche (IDiBE), Universidad Miguel Hernández (UMH), 03202 Elche, Spain
[b] Fish Pathology Group, Institute of Aquaculture Torre de la Sal — Spanish National Research Council (IATS-CSIC), 12595 Cabanes, Castellón, Spain

ARTICLE INFO

Keywords:
Electrospinning
Nanofibers
Proteins
Antimicrobial peptides
Antibody

ABSTRACT

In this study, the electrospinning procedure was optimized to create polyethylene oxide (PEO) NFs highly enriched in proteins with non-structural functions while preserving their activity. For this purpose, several immune-related proteins of low, medium and high molecular weights were used as molecular models. Initially, the electrospinning parameters were adjusted using 3 % *w*/w PEO and bovine serum albumin (BSA, 5–20 % *w*/w). As determined by FESEM, their average diameters ranged from 301 to 752 nm, and those with higher protein content (15–20 %) yielded more uniform NFs in both size and morphology terms. Protein integrity remained stable as determined by SDS-PAGE and FTIR. Similar results were observed for the polypeptide lysozyme (LYZ) when incorporated in NFs under these settings. To further explore the potential of these materials, the antimicrobial peptide piscidin (PIS) and an antibody (Ab, HRP-IgG) were used to produce BSA/PIS, LYZ/PIS and BSA/Ab NFs and evaluate the preservation of their activity. The antibacterial assays showed that, in most bacterial species, the activity of PIS remained consistent after being incorporated into the NFs. Furthermore, the activity of HRP-IgG was maintained within the NFs, with enhanced preservation observed in BSA/Ab NFs. These findings expand the possibilities of protein utilization across various applications through nanomaterials.

1. Introduction

Natural bioresources offer a vast array of protein structures, collectively representing a rich source of important, specific, and often unique bioactivities with potential for exploitation in various applications. Through dedicated research and development, there is a significant opportunity to harness these functionalities for the prevention, mitigation, and treatment of numerous medical conditions. In fact, the successful application of certain proteins in treating severe diseases has recently transformed the pharmaceutical and biotechnological industries, sparking growing interest in further advancements. As a consequence, there has been a significant increase in the number of protein-based drugs approved by the US Food and Drug Administration (FDA) in the last decades, reaching about 894 therapeutic proteins in 2024 as it is collected in the THPdb2 database of all FDA-approved therapeutic proteins [1], what implies nearly 4 times more than in its previous version, THPdb (239), released 7 years before [2].

Despite the promising potential of proteins as therapeutics and the growing advances in the field of biotechnology, several limitations reducing their therapeutic activity impede the progress of many candidates through industrial pipelines. Regardless of their route of administration, therapeutic proteins encounter common challenges that compromise their safety and efficacy, such as immunogenicity, low solubility, poor stability and short half-life. Additionally, their practical use and affordability are limited by factors like short shelf life and high costs. Therapeutic proteins intended for topical applications also face additional constraints such as inadequate skin absorption and lack of suitable delivery formats [3]. Innovative strategies such as chemical modifications of the active ingredients have contributed to notably meliorate some particular limitations, but attention is now focused on excipient development due to the recent multiple benefits provided by new forms and compositions of the overall delivery system formulation. For topical applications, besides the film-forming and ionic liquid systems [4], the implementation of nanocarriers or nano-delivery systems

* Corresponding authors.
E-mail addresses: alberto.falco@csic.es (A. Falcó), r.mallavia@umh.es (R. Mallavia).

https://doi.org/10.1016/j.ijbiomac.2024.136019
Received 30 July 2024; Received in revised form 13 September 2024; Accepted 23 September 2024
Available online 26 September 2024

(i.e., transporters which nanometric size confers them with new unique properties) has improved therapeutic performances of several drugs.

Among the different types of nanocarriers, polymeric nanofibers (NFs) offer several interesting therapeutic advantages for topical applications extensively discussed in the literature [5]. One common method for synthesizing polymeric NFs is electrospinning, a technique that produces fibers with controlled diameters and high surface area. As for any other nanomaterial, the high surface-to-volume ratio of NFs increases their loading capacity not only for the specific drug, but also for additional adjuvants. In the specific case of polymeric NFs, the molecular rearrangements inherent to the electrospinning process, together with the wide availability of different biocompatible polymers (and therefore physicochemical conditions), allow the encapsulation of poorly soluble compounds, as well as multiple design options to tune the release kinetics as desired. This versatility can also be used to enhance the protection and molecular stability of the content, thereby extending the shelf life of the formulation and increasing its commercial interest. Other advantages of this particular format include the ability of creating favorable physiological microenvironments functionally mimicking the natural extracellular matrix to enhance cell migration, attachment and proliferation and thus processes such as wound healing and hemostasis [6]. Finally, it is also remarkable that these nanoformulations allow more precise dosage control and ease of administration at the site of disease, which promotes therapeutic efficacy and patient compliance, as well as safe shelf management.

Despite these advantages, research on encapsulating therapeutic proteins in polymeric NFs remains both limited and often biased. A likely explanation for this is that the intricate structural complexity of many therapeutic proteins may be compromised during NF fabrication, either due to physicochemical conditions and/or direct interactions with the polymer or solvent. This, in turn, could impair their activity, as outlined by Anfinsen's dogma. Indeed, most studies in this field tend to focus on filamentous proteins, such as collagen [7] elastin [8], gelatin [9], keratin [10], and silk fibroin [11], whose structural roles are less dependent on their conformation. By contrast, for proteins with a more critical dependence on molecular structure-activity relationships, such as enzymes (e.g., lysozyme [12,13], lipase [14], and peroxidase [15]), or antibodies [16], their incorporation to NFs is typically achieved through covalent immobilization to the polymer used. Fewer studies have explored the free incorporation of these proteins into NFs, specially by electrospinning, and then assessed their activity. Among them, bovine serum albumin (BSA) stands out as one of the most extensively studied globular proteins, valued for its wide availability, low cost, and crucial role as a transporter and stabilizing agent. For instance, dressings of 11 % (*w*/w) polycaprolactone (PCL) NFs loaded with 1–3 % (w/w) BSA stimulated wound healing processes [17]. In another study, polyethylene oxide (PEO) (5 %, w/w) NFs with BSA (0.5 %, w/w) were produced by needleless electrospinning without altering the protein structure [18]. Lysozyme (hereafter referred to as LYZ), an important protein of the innate immune system with potent antimicrobial activity and which structure-activity relationship has been widely described [19], was also encapsulated (0.2 %, *w*/w relative to polymer mass) into NFs of PCL/PEO blends via emulsion electrospinning [20]. Remarkably, in this study it was demonstrated that the release of LYZ was facilitated by the hydrophilic nature of PEO, which enhanced the diffusion of water into the electrospun NFs [20].

PEO, also known as polyethylene glycol (PEG) for molecular weights below 20 kDa, is a commercially available polyether that comes in a wide range of molecular weights at relatively low cost. Its exceptional resistance to protein adsorption, along with poor cell adhesion and minimal toxicity and immunogenicity, has led to its approval by the FDA for various biomedical applications. Additionally, it offers high chemical stability and, importantly, high solubility in water [21], the ideal solvent (aqueous solutions) for therapeutic proteins. These properties make this polymer highly promising for the nanoencapsulation of therapeutic proteins; specifically, in the case of NFs, the higher molecular weight of PEO enhances polymer entanglement [22,23] and impermeability [24], thereby improving the stability of the resulting nanomaterial.

In this study, we aim to further explore this approach by testing the suitability of electrospun PEO NFs as a delivery vehicle for therapeutic proteins for potential biomedical applications. To this end, we begin by using BSA (approximately 66 kDa) to optimize the electrospinning parameters, allowing us to refine the fabrication of NFs with three proteins of quantifiable activity, spanning a wide range of molecular sizes and structural complexities: the antimicrobial peptide (AMP) piscidin 1 from European seabass (PIS, 2.6 kDa), chicken LYZ (14.3 kDa), and horseradish peroxidase (HRP)-conjugated goat anti-mouse IgG (HRP-IgG, nearly 200 kDa). Finally, after analyzing the integrity of the encapsulated proteins, we assess their activity in order to determine the retainment of activity after the full process.

2. Materials and methods

2.1. Materials

PEO (Mw = 600–1000 kg/mol), Standard Fetal Bovine Serum, Dulbecco's Modified Eagle Medium (DMEM) and Dulbecco's Phosphate Buffered Saline (PBS) were acquired from Thermo Fisher Scientific (Waltham, MA, USA). LYZ (chicken egg white, A3711,0050; Activity 20,780 U/mg) and 3-(4,5-dimethylthiazol-2-yl)-2,5-diphenyl tetrazolium bromide (MTT) were procured by Panreac, ITW Reagents (Barcelona, Spain). BSA (heat shock fraction, pH 7, purity >98 %; A7906-50G), p-iodonitrotetrazolium chloride (INT), Mueller Hinton (MH) agar and HRP-IgG, A5278) were obtained from Sigma-Aldrich (St. Louis, MO, USA). MH broth was provided by Condalab (Madrid, Spain). PIS (from European sea bass, accession # MT066191, C-terminal amidation and purity >90 %) was purchased from Genscript Biotech Corp (Piscataway, NJ, USA). Tetramethylbenzidine (TMB) was acquired from Bio-Rad Laboratories GmbH, Munich, Germany.

2.2. Preparation of solutions for electrospinning

2.2.1. Starting solutions and viscosity determination

Hereafter all concentrations expressed as percentages will be based on weight/weight (*w*/w), unless stated otherwise. PEO solutions with protein (BSA or LYZ) were obtained by dissolving 5 to 20 % protein and 3 % PEO in Milli-Q water (solvent compatible with both types of molecules, especially proteinic ones). All the solutions were kept stirring for 12 h until their complete dissolution and homogenization. The kinematic viscosity (ν) of all blend solutions was performed by using a series of calibrated Cannon-Fenske capillary viscometers series 400–450 (Vidra Foc, Barcelona, Spain) to elucidate their electrospinnability. Corresponding density (ρ) was measured with calibrated volumetric flask, in order to estimate their shear viscosity ($\eta = \nu\rho$ [mPa·s]). The average value of three measurements at 313 K was represented as mean and standard deviation (SD).

2.2.2. Peptide and antibody solutions

After optimization, an electrospinnable solution containing 15 % of total protein and 3 % of PEO was selected to add the peptide and antibody. The concentrations were chosen based on the minimum concentration added at which activity was observed. The chosen peptide was PIS, a small 22-residue antimicrobial peptide. PIS was added at 0.1 % in both BSA (BSA/PIS) and LYZ (LYZ/PIS) solutions to compare the antibacterial activity of both types of NFs. To assess the stability of larger and more complex proteins within the NF system studied here there were produced NFs loaded with peroxidase-conjugated antibody, in particular an HRP-IgG commonly used as secondary antibody for immunolabelling assays. HRP-IgG was added at 1 % in BSA solutions (BSA/Ab).

Table 1
Polymer (PEO) and protein content in the starting polymeric solutions and obtained NFs.

Polymeric solutions (*w*/w %)		Electrospun NFs (w/w %)	
PEO	Protein	PEO	Protein
3	5	37	63
	10	23	77
	15	17	83
	20	13	87

2.3. Electrospinning

The solutions were transferred to 2 mL syringes (Becton Dickinson, Franklin Lakes, NJ, USA) attached to a blunt-end stainless steel hypodermic needle (5 cm in length, outer diameter of 1.27 cm and inner diameter of 0.84 cm) (Sigma-Aldrich). Solutions were electrospun at a sustained flow controlled by a KDS 100 infusion pump (KD Scientific, Holliston, MA, USA) and using a high voltage source (Glassman High Voltage Inc., Whitehouse Station, NJ, USA) as previously described [25]. The optimization of the electrospinning conditions was a multi-step process involving the fine-tuning of both the polymer solution (i.e., by testing the concentration gradient described above) and the electrospinning parameters. The key parameters that were modified included the applied voltage, the tip-to-collector distance, and the flow rate. These parameters were systematically varied within the following ranges: voltage from 10 to 20 kV, tip-to-collector distance from 12 to 18 cm, and flow rate from 0.2 to 0.5 mL/h. These ranges were chosen based on our previous studies, some of which used water as a solvent [25,26]. Through this systematic variation, the optimal electrospinning conditions were determined to be an applied voltage of 18 kV, at a tip-to-collector distance of 17 cm, with a flow rate of 0.25 mL/h, always at 20–40 % relative humidity and 25 °C. These conditions were found to produce NFs with the most desirable morphology and size, including minimization of electrospray, small droplets and NF defects such as beads or ribbon-like structures. The obtained NFs were deposited in aluminum foil-coated glass slides. After the electrospinning process, which involved solvent evaporation, the protein and polymer content varied, as reflected in Table 1. The NFs were not further processed for subsequent analyses unless otherwise stated in the corresponding section.

2.4. Microscopy

NFs were initially screened using a Microsystems DMI3000B inverted fluorescence optical microscope (Leica, Bensheim, Germany) with a Leica EL6000 compact light source and a Leica DFC 3000G digital camera. The images were processed using the program Leica Application Suite AF 6000 Module Systems. The morphology and size of NFs were later analyzed by Field Emission Scanning Electron Microscopy (FESEM) with a Schottky cathode model SIGMA 300 VP (Zeiss, Oberkochen, Germany) apparatus after chrome metallization. The average diameter of different types of NFs was determined using Image J (National Institutes of Health) image processing and analysis software from 100 measurements for each type of NFs using different FESEM images. The coefficient of variation (CV) was calculated by dividing the SD by the mean.

2.5. Electrophoresis

The protein integrity after electrospinning was assessed by SDS-PAGE. NFs from 5 to 15 % protein solutions were dissolved back in water to reach 10 μg/μL protein concentrations, separated by SDS-PAGE (Bio-Rad Laboratories Inc., CA, USA) under denaturing conditions in 4–20 % TGX gels (Bio-Rad Laboratories Inc.), and visualized with Brilliant Blue R-250 (Bio-Rad Laboratories Inc.). Molecular weight markers (Precision Plus Protein Standards Dual Colour, Bio-Rad Laboratories Inc.) were loaded in the first well of the gel.

2.6. Infrared spectroscopy

Fourier transform infrared (FTIR) spectroscopy was performed to define the functional groups of all samples using a Spectrum Two™ FTIR spectrometer (PerkinElmer, MA, USA). PEO, BSA and LYZ powder samples were mixed with KBr and pressed into pellets. Nanofibrous mats were directly measured. Four spectral scans in transmission mode were averaged throughout the spectral range of 4000–450 cm^{-1} with the resolution of 4 cm^{-1} at room temperature.

2.7. Antibacterial evaluation

Aeromonas salmonicida (CECT 894), *Bacillus circulans* (CECT 10), *Bacillus subtilis* (CECT 35), *Escherichia coli* (CECT 45), *Micrococcus luteus* (CECT 243) and *Staphylococcus epidermidis* (CECT 231) bacterial species were obtained from the Spanish Type Culture Collection (CECT, Valencia, Spain). *S. aureus* and MRSA were obtained from clinical samples of patients at the General University Hospital of Alicante. Bacteria were cultured in MH broth and incubated at 30 or 37 °C for 24 or 48 h, depending on the species optimal growth conditions.

Antibacterial activity of commercial LYZ and PIS, and LYZ/PIS and BSA/PIS NFs was determined by broth microdilution method by minimum inhibitory concentration (MIC) and minimum bactericidal concentration (MBC) calculation. The pure compounds or the NF mats were first dissolved in Milli-Q water and filtered using sterile CA syringe filters with pore size of 0.22 μm. 50 μL were added in 96-well plates at different concentrations depending on the sample. A bacterial suspension of 20 μL at 0.5 McFarland were added to each well. The volume of each well was brought to 200 μL by adding MH broth. The plates were incubated at 30 or 37 °C for 24 or 48 h depending on the strain. A volume of 50 μL of INT solution at 1 mg/mL was added to each well and allowed to incubate for 30 min. The MIC was defined as the minimum concentration where no red colour was observed. To determine the MBC, 50 μL of the wells that did not show any signs of bacterial growth were plated and incubated overnight on MH agar plates. The lowest concentration at which no colonies were detected was defined as the MBC.

2.8. Peroxidase activity of encapsulated HRP

Stored samples of HRP-IgG-containing NFs were dissolved back in Tris-buffered saline (TBS) to reach a final 1:500 dilution of the initial HRP-IgG stock or equivalently in the case of control NFs without HRP-IgG. Two-folded serial dilutions were subsequently prepared from these samples up to 1:16000 dilution. Equivalent dilutions of the fresh HRP-IgG were also prepared to serve as positive control and calibration curve. Then, 5 μL of each were inoculated into MaxiSorp™ 96-well plates (NUNC, Rochester, NY, USA) in triplicate and incubated with additional 95 μL of TMB substrate commercial solution for 30 min at 37 °C in the dark.

Finally, the reaction was stopped with 50 μL of 1 N H_2SO_4, and the absorbance measured at 450 nm using an UltraEvolution automatic plate reader (Tecan, Männedorf, Switzerland).

2.9. Antigen-recognition activity of encapsulated IgG

The assessment of the viability of the encapsulated HRP-IgGs was carried by adapting a direct ELISA procedure. Thus, MaxiSorp™ 96-well plates were coated with 50 μL of a 1:4 dilution of an in-house hybridoma supernatant in TBS containing 0.4 mg/ml of protein as determined using a Nanodrop 2000c (Thermo Scientific, Wilmington, DE, USA), and incubated overnight at 4 °C. After three washes of 5 min with 200 μ-L TBS supplemented with 0.05 % (*v*/v) Tween-20 (TTBS) and one with

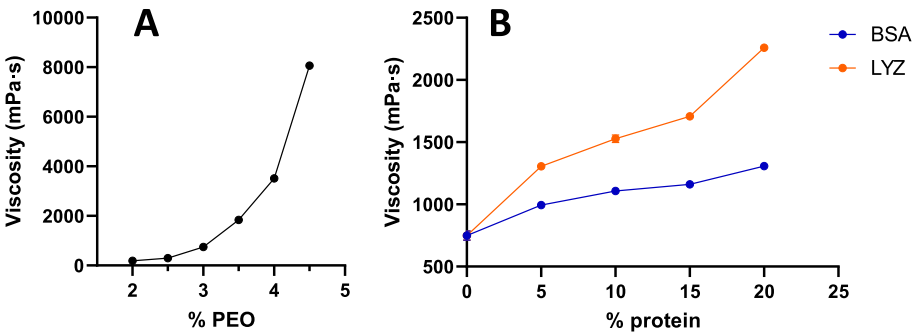

Fig. 1. Viscosity of polymeric solutions containing different concentrations of PEO (A), and containing 3 % PEO and different concentrations of BSA and LYZ (B). Relative error < 5 % for $n = 3$.

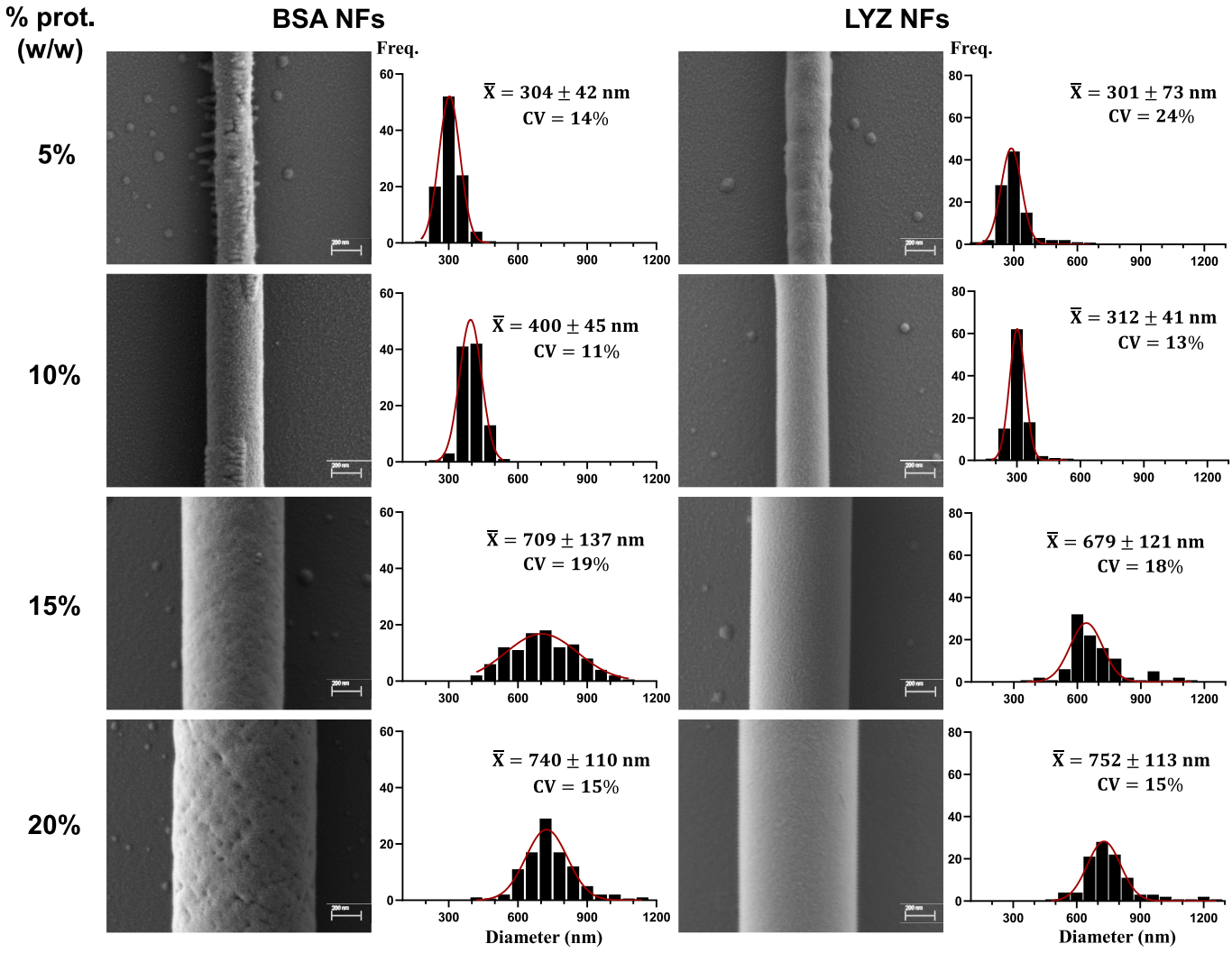

Fig. 2. FESEM images and diameter frequency histograms of electrospun NFs containing PEO and different concentrations of BSA and LYZ. Representative FESEM micrographs and corresponding diameter frequency histograms for BSA (5–20 %) and LYZ (5–20 %) are shown. Prot. refers to the BSA and LYZ proteins, as appropriate. Histogram data were obtained from multiple micrographs (100 individual measurements). Best-fit adjustments to a Gaussian distribution are indicated in red. Average diameter (X) ± SD, as well as coefficient of variation (CV, %) are also stated. Scale bar: 200 nm. (For interpretation of the references to colour in this figure legend, the reader is referred to the web version of this article.)

TBS, plates were blocked with 100 μL of 1 % (*w/v*) BSA in TBS for 1 h at 37 °C. Subsequently, the washing steps were repeated and 50 μL of each dilution of the dissolved NFs and corresponding control samples described above were added. Plates were incubated at 37 °C for 1 h and washed again. Finally, the reaction with TMB substrate (100 μL/well) and the absorbance measurement were carried out as described above.

2.10. Data analysis

All experimental data are expressed as mean values ± SD. Data

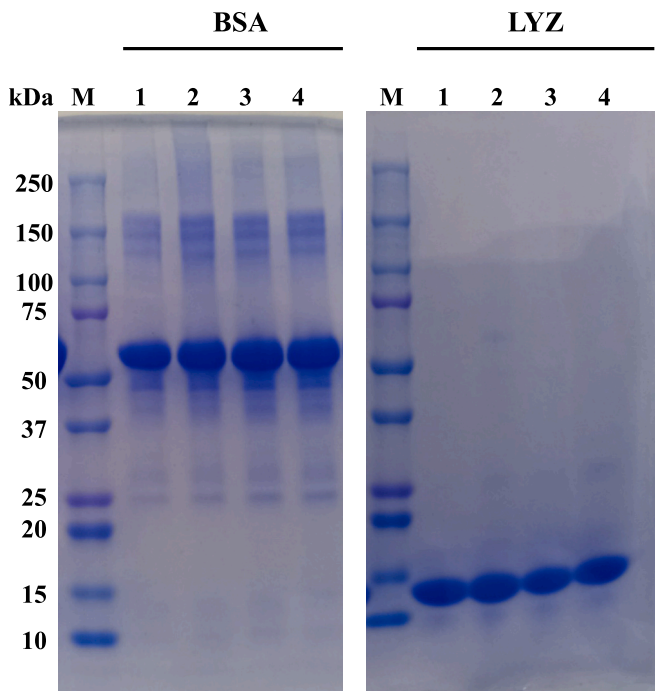

Fig. 3. SDS-PAGE results of BSA (left) and LYZ (right) NFs. In each lane, NFs corresponding to 10 μg of protein were loaded. M: marker; Lane 1: protein (BSA or LYZ) control; lane 2: 5 % protein NFs; lane 3: 10 % protein NFs; lane 4: 15 % protein NFs; M: marker.

manipulation, analysis and graph creation were carried out using Prism v8 software (GraphPad software, La Jolla, CA, USA), depending on each particular experimental design.

3. Results

3.1. Solution viscosity and electrospinning

Firstly, the viscosity of different PEO solutions at concentrations ranging from 2 to 5 % was evaluated to determine the optimal concentration for NFs formation and their molecular weight. The viscosity of PEO solutions increased with concentration and ranged from 189 ± 3 mPa·s at 2 % to 8060 ± 113 mPa·s at 5 % (Fig. 1A). In basis on these viscosity results, the nominal molecular weight of PEO was estimated around 580–620 kg/mol.

Only PEO solutions with a concentration of 4 % or higher (viscosity of 3515 ± 25 mPa·s) were able to form continuous NFs without beads. Although the 3 % PEO solution (viscosity of 749 ± 37 mPa·s) was not able to form fibers on its own, when the protein was added at concentrations of 5 to 20 %, it was able to be electrospun. Therefore, a 3 % concentration of the building polymer was chosen to synthesize the protein NFs. Fig. 1B shows the viscosities of the BSA and LYZ solutions, which increased with protein concentration.

3.2. Morphology of nanofibers

The morphology of the electrospun NFs was analyzed using FESEM. Fig. 2 displays both the detailed FESEM images and the frequency histograms of the diameter distribution of the NFs of BSA and LYZ at different concentrations. The general images of the NFs at lower magnification can be observed in Supplementary Fig. 1.

As can be observed in Fig. 2, the diameter of the NFs increased with increasing protein concentration and CVs were within the range of 11–24 % in both cases. The appearance of the NFs from 15 and 20 % of protein solutions (BSA and LYZ) was smooth and uniform, without any visible deformities or irregularities. However, the NFs produced from 5 % solutions, especially 5 % BSA NFs, displayed certain irregularities such as small droplets, fused fibers or beads. Based on these results, the 15 % protein solutions were selected to further functionalize this NFs, as it was the lowest concentration at which no fused NFs, deformations, or excessive electrospray were observed.

3.3. Protein integrity

SDS-PAGE was conducted to verify that the proteins have not undergone alterations affecting their size, such as degradative processes or covalently stabilized aggregations, as these could have implications for their activity. To do so, the amount of protein present in the NFs was estimated and normalized to the same amount of protein. Fig. 3 shows the bands revealed in the gels with BSA and LYZ NFs. It was found that the electrophoretic mobility of the electrospun BSA and LYZ NFs was equivalent to that of the commercially available BSA and LYZ. The gel analysis of BSA NFs revealed a consistent molecular weight of approximately 65 kDa in all lanes, which corresponds to the expected molecular weight of BSA (lane 1). The band density observed in lanes 2–5 was around 100 % compared to the control protein (lane 1). On the other hand, for LYZ gel, the molecular weights of all lanes were approximately 12 kDa, consistent with the expected molecular weight of LYZ (lane 1), and the band densities in lanes 2–4 were also close to 100 % compared to lane 1 or LYZ control.

The FTIR spectra of the electrospun NFs were obtained to investigate their chemical composition and are shown in Fig. 4, together with their starting components prepared in pellets. Hence, they exhibit characteristic bands of the base polymer (PEO) corresponding to the frequencies 1103 cm^{-1} (C-O-C stretching) and 956 and 840 cm^{-1} (asymmetric CH_2 rocking motion). These spectral features were also discernible in the spectra of the NFs containing proteins, as depicted in the inset of the spectral figures.

Furthermore, there is no discernible alteration in the amide bands of the native proteins under investigation (BSA and LYZ). In both cases, the predominant presence of these proteins in the NFs closely resembles that observed in the unprocessed source material. Consequently, the stability and constancy of amide I at 1657 cm^{-1}, as well as amide A, amide II, and amide III (at 3303 cm^{-1}, 1540 cm^{-1}, and 1240 cm^{-1}, respectively) is noteworthy.

Finally, the integrity of the LYZ NFs was also evaluated in terms of maintaining their antibacterial activity. Initially, a screening of commercial LYZ against all bacteria used in this study was conducted, and it was observed that it was only capable of inhibiting *B. circulans*. Subsequently, the antibacterial capacity of the LYZ NFs (5–20 %) was evaluated, and it was observed that the antibacterial activity was maintained at the same level as the free LYZ (Supplementary Table 1).

3.4. Preparation of PIS NFs and determination of antibacterial activity

First, a screening of the antibacterial activity of PIS against Gram-negative bacteria *A. salmonicida* and *E. coli*, and Gram-positive bacteria *B. circulans*, *B. subtilis*, *M. luteus*, *S. aureus* (including MRSA) and *S. epidermidis* was conducted, and it was able to inhibit all tested bacteria. Therefore, PIS was incorporated into both BSA and LYZ NFs. The synthesized NFs can be observed in Fig. 5. In both cases, the NFs were uniform, and the diameters were 625 ± 58 nm for the BSA/PIS NFs and 618 ± 73 nm for the LYZ/PIS NFs. FESEM images of the NFs at lower magnification can be found in Supplementary Fig. 2.

Subsequently, the antibacterial potential of BSA/PIS and LYZ/PIS NFs against all bacterial species was assessed. Table 2 shows the results of the 96-well microdilution assays of the free PIS and the proportional part to the PIS of the BSA/PIS and LYZ/PIS NFs.

In this study, free PIS was capable to inhibit all bacteria tested with MIC values ranging 3.9–15.6 μg/mL and MBC from 7.8 to 62.5 μg/mL. Regarding the BSA/PIS and LYZ/PIS NFs, all of them also showed

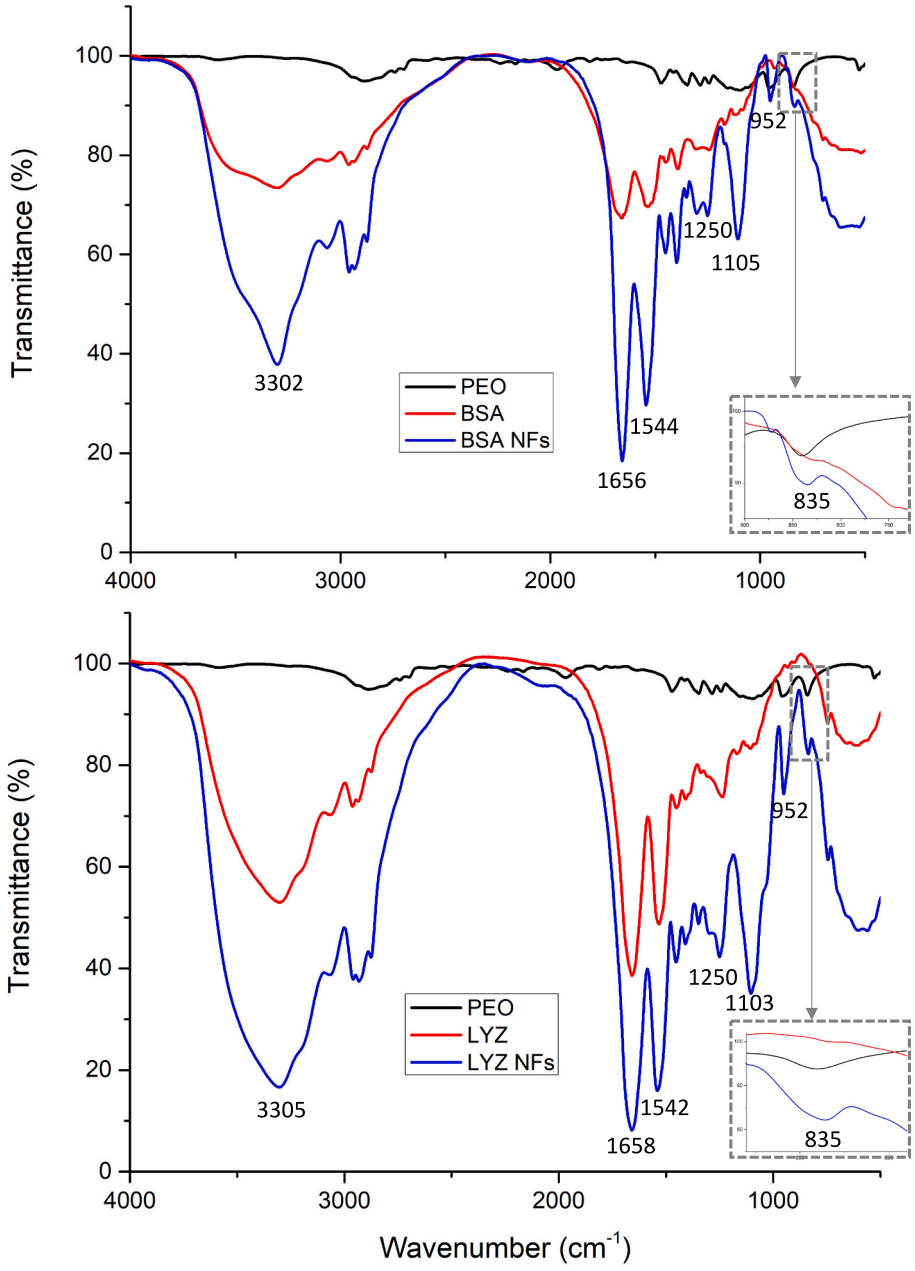

Fig. 4. FTIR spectra of BSA, PEO and BSA/PEO NFs (top) and LYZ, PEO and LYZ/PEO NFs (bottom). The PEO and unprocessed protein samples were prepared into KBr pellets. The NFs were prepared from 15 % protein and 3 % PEO solutions, and the mats were measured in their unprocessed state. Inset: enlarged detail of 840 cm^{-1} band corresponding to the PEO asymmetric CH_2 rocking motion.

antibacterial activity against all tested bacteria. In bacterial species *M. luteus*, *S. aureus*, MRSA and *S. epidermidis*, the MIC remained unchanged. However, in *A. salmonicida*, *B. circulans*, *B. subtilis* and *E. coli*, both the MIC and the MBC were increased, especially in the BSA/PIS NFs. Additionally, in most cases, the activity of the LYZ/PIS NFs was greater than that of the BSA/PIS NFs, even surpassing that of the free PIS in some species, as highlighted in bold in Table 2.

3.5. Preparation of Ab NFs and activity analysis of peroxidase-conjugated antibody

To test the feasibility of the system with larger and more complex proteins with non-structural functions, the repertoire of proteins to be encapsulated was extended. A commercial combination of peroxidase and antibody, i.e., HRP-IgG, was incorporated into the BSA NFs. Fig. 6 displays an image of the synthesized BSA/Ab NFs as well as the frequency histogram of diameters. The synthesized NFs were homogeneous, with an average diameter of 513 ± 70 nm. Supplementary Fig. 3 shows general images of these NFs at lower magnification.

PEO and PEO/BSA NFs with HRP-IgG and without HRP-IgG (control) were used to test the retained activity of HRP-IgG. After 1 month of storage at −20 °C, NFs were dissolved in TBS to a final dilution of 1:500 of the initial HRP-IgG stock, or an equivalent volume for control NFs, and 2-fold serially diluted up to 5 times. The retained peroxidase activity in these samples was then determined together with corresponding dilutions of the HRP-IgG fresh stock, which was found to adjust to a linear correlation ($Y = 1963\times$ - 0.02739; $R^2 = 0.9979$) (Fig. 7A). Thus, it is observed that, in comparison to HRP-IgG controls, the peroxidase activity of the HRP was reduced up to 7.4 ± 0.5 folds in NFs without BSA, but just only about 4 folds (precisely, 3.9 ± 0.26) in BSA NFs, meaning a

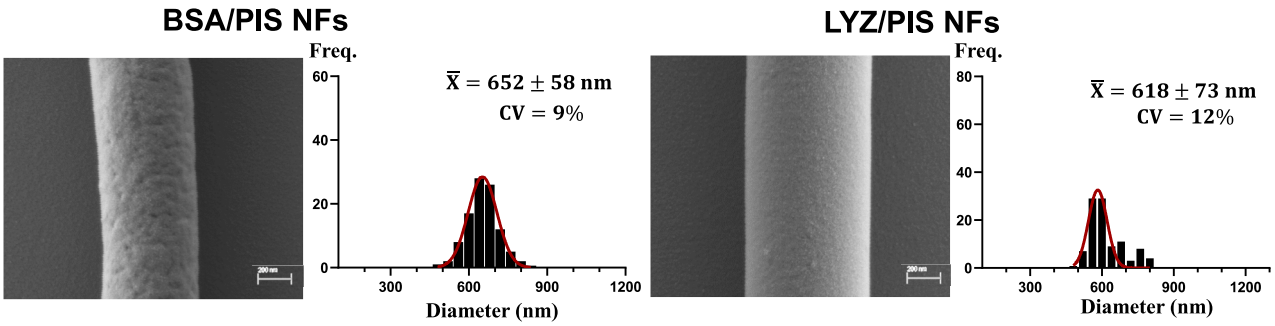

Fig. 5. FESEM images and diameter frequency histograms of BSA/PIS (left) and LYZ/PIS (right) electrospun NFs. Histogram data were obtained from multiple micrographs (100 individual measurements). Best-fit adjustments to a Gaussian distribution are indicated in red. Average diameter (X) ± SD, as well as coefficient of variation (CV, %) are also stated. Scale bar: 200 nm. (For interpretation of the references to colour in this figure legend, the reader is referred to the web version of this article.)

Table 2
Minimum inhibitory concentration (MIC) and minimum bactericidal concentration (MBC) of commercial PIS and the proportion of PIS contained in the BSA/PIS and LYZ/PIS NFs against *A. salmonicida, B. circulans, B. subtilis, E. coli, M. luteus, S. aureus*, MRSA and *S. epidermidis.*

0g	MIC (μg/mL)			MBC (μg/mL)		
	PIS	BSA/PIS NFs	LYZ/PIS NFs	PIS	BSA/PIS NFs	LYZ/PIS NFs
A. salmonicida	7.8	31.3	7.8	15.6	249.6	15.6
B. circulans	15.6	62.6	**5.0**	15.6	249.6	**7.8**
B. subtilis	15.6	31.3	**7.8**	31.3	62.6	31.3
E. coli	31.3	62.6	31.3	62.6	124.8	124.8
M. luteus	15.6	15.6	**7.8**	31.3	124.8	62.6
S. aureus	31.3	31.3	31.3	62.6	62.6	62.6
MRSA	15.6	15.6	**7.8**	31.3	31.3	31.3
S. epidermidis	3.9	3.9	**2.0**	7.8	7.8	**2.0**

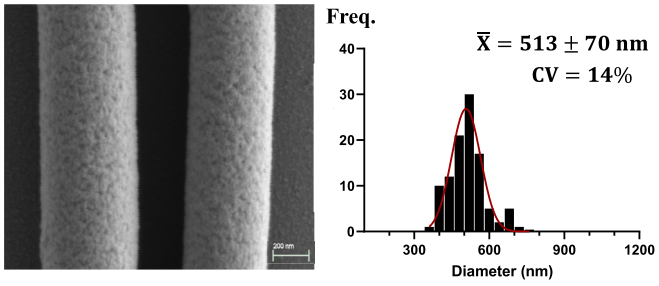

Fig. 6. FESEM image and diameter frequency histogram of BSA/Ab electrospun NFs. Histogram data were obtained from multiple micrographs (100 individual measurements). Best-fit adjustments to a Gaussian distribution are indicated in red. Average diameter (X) ± SD, as well as coefficient of variation (CV, %) are also stated. Scale bar: 200 nm. (For interpretation of the references to colour in this figure legend, the reader is referred to the web version of this article.)

residual activity of 13.5 ± 0.9 % and 25.7 ± 1.7 %, respectively.

Considering this result, in a follow-up ELISA assay targeting mouse IgG detection using these samples (Fig. 7B), obtaining lower signals relative to the peroxidase activity would indicate a reduced epitope recognition activity of the antibody. However, this was not the case for NFs with BSA and encapsulated HRP-IgG. At least three dilutions from these samples showed signals above the assay's detection limit (0.0147 ± 0.003 a.u. of A_{450}). On average, these NFs retained 31.9 ± 0.9 % of their activity compared to controls (which adjusted to a quadratic correlation: $Y = 71854 \times ^{2} + 199.3\times$ - 0.0247; $R^2 = 0{,}9989$). For the NFs without BSA, only the lowest dilution (1:500) gave a signal within the detection limit of the assay (0.0111 ± 0.0042 a.u. of A_{450}). The average activity retention of HRP-IgG from these NFs was 8.5 ± 0.9 % compared to the control.

4. Discussion

This study represents the first report on the production and characterization of NFs with high content of two non-structural proteins, i.e., BSA and LYZ. To date, BSA and LYZ have been incorporated into NFs in combination with PEO in certain studies [17,27,28]. Nevertheless, in most of these studies, they have been utilized in limited amounts as model proteins to examine drug release, rather than serving as the primary constituent of the NFs. PEO was selected as the copolymer based on previous studies that identified PEO (nominal 600 kg/mol PEO) as an interesting polymer for electrospinning due to its optimal biocompatibility and biodegradability properties [18].

The present study has identified viscosity of the solutions as a crucial factor in the formation of NFs. Previous reports have also highlighted the notable impact of viscosity on morphology and size during the electrospinning process [29]. Some studies indicate that viscosity ranges of 300 to 2000 mPa·s in polymeric PEO solutions are considered appropriate for electrospinning [29–31]. However, the optimal viscosity range may differ based on the specific conditions and electrospinning setup being utilized. As shown in Fig. 1, viscosity increased with protein concentration and LYZ solutions showed higher viscosity than BSA solutions, which could be attributed to the repulsion that PEO induces between LYZ molecules [32], leading in turn to an increase in resistance to flow [33]. Another notable aspect is that the viscosities of all electrospinnable protein solutions are below 2300 mPa·s. However, PEO solutions with such viscosities were not able to be electrospun. This suggests that the addition of proteins can significantly improve the electrospinnability of the PEO solutions, acting as stabilizing agents. The addition of proteins in electrospinning solutions has been shown to increase conductivity [34], which in turn can enhance the uniformity of the electrospun fibers [35].

The NFs from solutions with lower protein concentration displayed certain defects, such as small droplets, which could be attributed to a combination of electrospraying and electrospinning, possibly resulting from the low viscoelasticity of the solution [36]. Overall, all NFs showed uniformity in diameter, as confirmed by CVs. A low CV suggests that there is less variation and greater consistency in a measured characteristic. Normally, a CV above 30 % indicates a high variability and therefore issues in the experiment [37]. In this case, all calculated CVs were within the range of 11–24 %, indicating high similarity in diameters within each sample.

The structure of the proteins within the NFs remained intact, as confirmed by SDS-PAGE and FTIR spectroscopy studies. Specifically, the electrophoretic mobility of the samples indicates that the proteins did not undergo any significant molecular conformation alterations during the electrospinning and solution preparation processes, as there were no

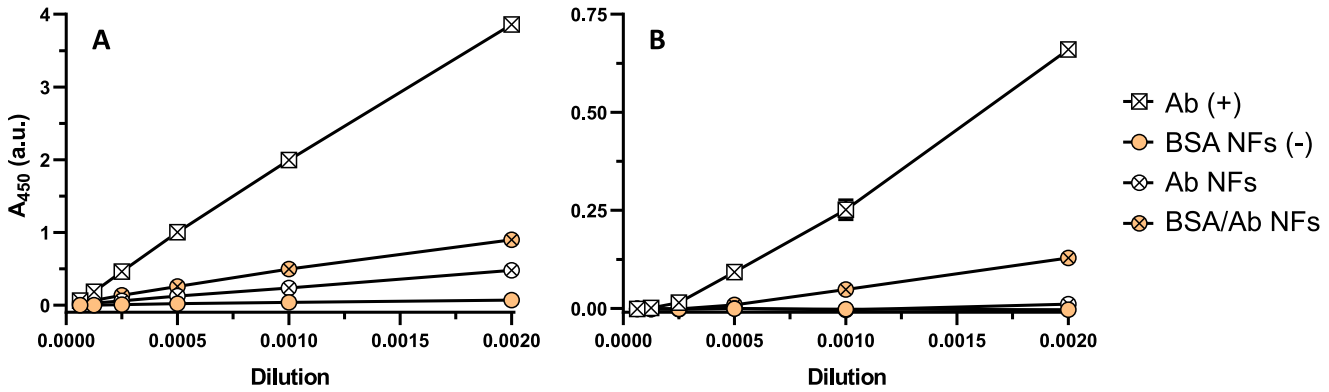

Fig. 7. Peroxidase and antigen-recognition activity of NF-encapsulated HRP-IgG. Two-fold serial dilutions starting in 1:500 (i.e., 0.002 dilution) of experimental and control samples were tested for enzymatic peroxidase (A) and antigen-recognition (B) activity. Represented sample groups include HRP-IgG as positive control (Ab (+)), and BSA/PEO (negative control, BSA NF (−)), HRP-IgG-loaded PEO (Ab NF), and HRP-IgG-loaded BSA/PEO (BSA-Ab NF) NFs. Data is presented as means ± SD of absorbance values at 450 nm in arbitrary units (A_{450}, a.u.) from representative experiments, each performed in triplicate.

significant indications of aggregation or hydrolysis [38]. On the other hand, the FTIR spectroscopy results showed distinct peaks for PEO, BSA, and LYZ, which agreed with previous findings [17,39]. BSA and LYZ NFs also exhibited these characteristic peaks, confirming the correct incorporation of protein in the NFs and indicating that the protein was not significantly altered during the electrospinning process. Finally, the structure of LYZ also demonstrated its preservation within the NFs, as the antibacterial activity was maintained at comparable levels to those of the free protein.

Once the integrity and stability of the synthesized NFs were demonstrated, the potential of these platforms as encapsulation and preservation systems for bioactive compounds was explored. To this end, proteins from the immune system with specific functions whose activities were easily evaluable were selected.

PIS was chosen for its loading into NFs due to its potent antimicrobial activity and because its incorporation into NFs had not been previously described. Its inclusion was carried out in both BSA and LYZ NFs to determine if there were differences in the antibacterial activity when evaluating it alongside a protein with and without activity. The NFs synthesized with PIS, i.e., BSA/PIS and LYZ/PIS, showed homogeneity and diameters of 625 ± 58 nm and 618 ± 73 nm, respectively. Their antibacterial activity was determined against pathogenic bacteria and an antibiotic-resistant bacteria (MRSA). The results obtained with free PIS are consistent with studies conducted by Pan et al., where MICs ranging from 3 to 50 μg/mL were obtained against Gram-negative bacteria [40]. Regarding the activity of the BSA/PIS and LYZ/PIS NFs, the MICs were calculated taking into account the proportion of PIS present in the NFs. It was observed that all NFs showed antibacterial activity, to a greater or lesser extent. In some species, the activity decreased compared to the free PIS, especially in the BSA/PIS NFs, with a higher MIC or MBC being observed. The lower activity observed in BSA/PIS NFs may be related to the use of BSA as a protective agent in NFs, aiding in the controlled and sustained release of drugs and thus preventing their initial burst releases [41,42]. In some other bacterial species, it was observed that the MIC or MBC of LYZ/PIS NFs was lower than that of BSA/PIS or even free PIS, even though these bacteria were not susceptible to LYZ. This suggests a potential synergy between LYZ and PIS, which could be a promising avenue for future research.

So far, the potentially therapeutic proteins incorporated into the NF system developed here have been of low/medium molecular weight, and therefore with relatively simple and renaturable higher structures (i.e., secondary and tertiary). Consequently, it was decided to incorporate more complex proteins, such as antibodies, specifically the HRP-IgG antibody. This strategy also allowed the evaluation of both the enzymatic and antigen recognition activity of a protein complex that is larger (almost 200 kDa) than its components (about 44 kDa for HRP and 150 kDa for IgG).

Based on the results obtained, NFs without BSA exhibited a significant decrease in both peroxidase activity and epitope recognition, possibly attributed to antibody denaturation occurring during electrospinning or storage [43,44]. Conversely, the inclusion of BSA in NFs appears to suggest a potential protective effect on the peroxidase activity of HRP-IgG. Despite the reduced peroxidase activity, the epitope recognition of the antibody in NFs with BSA remained relatively intact. This observation aligns with the well-documented stabilizing properties of BSA, which can act to prevent enzyme inactivation and protect proteins from unfolding or degradation [45,46]. The inclusion of BSA within the NFs likely creates a more favorable microenvironment for HRP-IgG, mitigating the potential stresses of encapsulation and storage. Future studies will focus on this direction, as well as on tuning the polymer composition to optimize the release kinetics, with special attention to the potential synergistic effects of blends of PEO and other polymers. Such modifications could pave the way for improved control over the release profiles, which is critical for applications in drug delivery.

5. Conclusions

The study successfully synthesized BSA and LYZ NFs as stable encapsulation platforms based on high protein amounts. Besides facilitating electrospinning, this platform serves as a stabilization system for the incorporation of other bioactive compounds. The uniform appearance of proteins in the NFs, as well as their structural integrity, which remained intact even at higher concentrations, indicate the potential of the synthesized NFs for effective biomedical applications. The antibacterial activity of PIS was generally maintained compared to free PIS, with LYZ/PIS NFs being more active than BSA/PIS NFs. The Ab activity was preserved in the NFs incorporating HRP-IgG, with preservation being notably higher in the NFs containing BSA. These findings support the viability of NFs as platforms for bioactive drug administration, highlighting their ability to maintain biological activity while enhancing stability.

CRediT authorship contribution statement

Rocío Díaz-Puertas: Writing – original draft, Visualization, Validation, Methodology, Investigation, Formal analysis, Data curation. **Enrique Rodríguez-Cañas:** Software, Formal analysis. **María Jesús Lozoya-Agulló:** Visualization, Investigation. **Pedro Valentín Badía-Hernández:** Investigation, Data curation. **Francisco Javier Álvarez-Martínez:** Writing – review & editing, Validation, Resources. **Alberto Falcó:** Writing – review & editing, Supervision, Methodology,

Investigation, Formal analysis, Conceptualization. **Ricardo Mallavia:** Writing – review & editing, Validation, Supervision, Resources, Project administration, Conceptualization.

Declaration of competing interest

The authors declare that they have no known competing financial interests or personal relationships that could have appeared to influence the work reported in this paper.

Data availability

Data will be made available on request.

Acknowledgements

This work was supported by the State Plan for Scientific and Technical Research and Innovation [Proyectos de Generación de Conocimiento, grant number PID2021-123253OB-C21], EU-FEDER [grant number GVA-IDIFEDER/2018/020, "*Una forma de hacer Europa*"], FEDER/Spanish Ministry of Science, Innovation and Universities—State Agency of Research [grant number RTI2018-101969-J-I00], the European Maritime, Fisheries and Aquaculture Fund (EMFAF) and the Ministry of Agriculture, Fisheries and Food (MAPA) [grant number MetDisFish], and Spanish Ministry of Science and Innovation—State Agency of Research with funding from NextGeneration EU [Proyectos de Consolidación Investigadora 2023, grant number CNS2023-145412].

We would like to extend our heartfelt gratitude to the administrative and technical support staff whose unwavering assistance was invaluable in the completion of this research project.

Appendix A. Supplementary data

Supplementary data to this article can be found online at https://doi.org/10.1016/j.ijbiomac.2024.136019.

References

[1] S. Jain, S. Gupta, S. Patiyal, G.P.S. Raghava, THPdb2: compilation of FDA approved therapeutic peptides and proteins, Drug Discov. Today 29 (7) (2024) 104047.
[2] S.S. Usmani, G. Bedi, J.S. Samuel, S. Singh, S. Kalra, P. Kumar, A.A. Ahuja, M. Sharma, A. Gautam, G.P.S. Raghava, THPdb: database of FDA-approved peptide and protein therapeutics, PLoS One 12 (7) (2017) e0181748.
[3] S. Bhawani Ahmad, A. Husaini, F. Ahmad Badruddin, M. Asaruddin Razip, Polymer based protein therapeutics, Curr. Protein Pept. Sci. 19 (10) (2018) 972–982.
[4] F. Iliopoulos, B.C. Sil, C.L. Evans, The role of excipients in promoting topical and transdermal delivery: current limitations and future perspectives, Frontiers in Drug Delivery 2 (2022).
[5] N. Raina, R. Rani, V.K. Thakur, M. Gupta, New insights in topical drug delivery for skin disorders: from a nanotechnological perspective, ACS Omega 8 (22) (2023) 19145–19167.
[6] Y. Ji, W. Song, L. Xu, D.-G. Yu, S.W. Annie Bligh, A review on electrospun poly (amino acid) nanofibers and their applications of hemostasis and wound healing, Biomolecules 12 (6) (2022) 794.
[7] J.X. Law, L.L. Liau, A. Saim, Y. Yang, R. Idrus, Electrospun collagen nanofibers and their applications in skin tissue engineering, J. Tissue Eng. Regen. Med. 14 (6) (2017) 699–718.
[8] I. González de Torre, A. Ibáñez-Fonseca, L. Quintanilla, M. Alonso, J.-C. Rodríguez-Cabello, Random and oriented electrospun fibers based on a multicomponent, in situ clickable elastin-like recombinamer system for dermal tissue engineering, Acta Biomater. 72 (2018) 137–149.
[9] H. Samadian, S. Zamiri, A. Ehterami, S. Farzamfar, A. Vaez, H. Khastar, M. Alam, A. Ai, H. Derakhshankhah, Z. Allahyari, A. Goodarzi, M. Salehi, Electrospun cellulose acetate/gelatin nanofibrous wound dressing containing berberine for diabetic foot ulcer healing: in vitro and in vivo studies, Sci. Rep. 10 (1) (2020) 8312.
[10] E. Serag, A.M.A. El-Aziz, A. El-Maghraby, N.A. Taha, Electrospun non-wovens potential wound dressing material based on polyacrylonitrile/chicken feathers keratin nanofiber, Sci. Rep. 12 (1) (2022) 15460.
[11] B.-M. Min, G. Lee, S.H. Kim, Y.S. Nam, T.S. Lee, W.H. Park, Electrospinning of silk fibroin nanofibers and its effect on the adhesion and spreading of normal human keratinocytes and fibroblasts in vitro, Biomaterials 25 (7) (2004) 1289–1297.
[12] P. Bayazidi, H. Almasi, A.K. Asl, Immobilization of lysozyme on bacterial cellulose nanofibers: characteristics, antimicrobial activity and morphological properties, Int. J. Biol. Macromol. 107 (2018) 2544–2551.
[13] J.-M. Park, M. Kim, H.-S. Park, A. Jang, J. Min, Y.-H. Kim, Immobilization of lysozyme-CLEA onto electrospun chitosan nanofiber for effective antibacterial applications, Int. J. Biol. Macromol. 54 (2013) 37–43.
[14] S.-F. Li, J.-P. Chen, W.-T. Wu, Electrospun polyacrylonitrile nanofibrous membranes for lipase immobilization, J. Mol. Catal. B Enzym. 47 (3) (2007) 117–124.
[15] R. Fazel, S.-F. Torabi, P. Naseri-Nosar, S. Ghasempur, S.-O. Ranaei-Siadat, K. Khajeh, Electrospun polyvinyl alcohol/bovine serum albumin biocomposite membranes for horseradish peroxidase immobilization, Enzym. Microb. Technol. 93-94 (2016) 1–10.
[16] G. Atik, N.M. Kilic, N. Horzum, D. Odaci, S. Timur, Antibody-conjugated electrospun nanofibers for electrochemical detection of methamphetamine, ACS Appl. Mater. Interfaces 15 (20) (2023) 24109–24119.
[17] S. Homaeigohar, M. Monavari, B. Koenen, A.R. Boccaccini, Biomimetic biohybrid nanofibers containing bovine serum albumin as a bioactive moiety for wound dressing, Mater. Sci. Eng. C 123 (2021) 111965.
[18] R. Ramakrishnan, J. Gimbun, P. Ramakrishnan, B. Ranganathan, S.M.M. Reddy, S. Ganesh, Effect of solution properties and operating parameters on needleless electrospinning of poly(ethylene oxide) nanofibers loaded with bovine serum albumin, Curr. Drug Deliv. (2019) 913–922.
[19] D.M. Chipman, N. Sharon, Mechanism of lysozyme action, Science 165 (3892) (1969) 454–465.
[20] T. Briggs, T.L. Arinzeh, Examining the formulation of emulsion electrospinning for improving the release of bioactive proteins from electrospun fibers, J. Biomed. Mater. Res. A 102 (3) (2014) 674–684.
[21] S. Zalipsky, J.M. Harris, Introduction to Chemistry and Biological Applications of Poly(ethylene glycol), Poly(ethylene glycol), American Chemical Society, 1997, pp. 1–13.
[22] W.W. Graessley, The Entanglement Concept in Polymer Rheology, the Entanglement Concept in Polymer Rheology, Springer, Berlin Heidelberg, Berlin, Heidelberg, 1974, pp. 1–179.
[23] H. Nie, A. He, W. Wu, J. Zheng, S. Xu, J. Li, C.C. Han, Effect of poly(ethylene oxide) with different molecular weights on the electrospinnability of sodium alginate, Polymer 50 (20) (2009) 4926–4934.
[24] S.L. Liu, L. Shao, M.L. Chua, C.H. Lau, H. Wang, S. Quan, Recent progress in the design of advanced PEO-containing membranes for CO2 removal, Prog. Polym. Sci. 38 (7) (2013) 1089–1120.
[25] A. Mira, C.R. Mateo, R. Mallavia, A. Falco, Poly(methyl vinyl ether-alt-maleic acid) and ethyl monoester as building polymers for drug-loadable electrospun nanofibers, Sci. Rep. 7 (1) (2017) 17205.
[26] A. Mira, C. Sainz-Urruela, H. Codina, S.I. Jenkins, J.C. Rodriguez-Diaz, R. Mallavia, A. Falco, Physico-chemically distinct nanomaterials synthesized from Derivates of a poly(anhydride) diversify the Spectrum of loadable antibiotics, Nanomaterials 10 (3) (2020) 486.
[27] H. Jiang, Y. Hu, Y. Li, P. Zhao, K. Zhu, W. Chen, A facile technique to prepare biodegradable coaxial electrospun nanofibers for controlled release of bioactive agents, J. Control. Release 108 (2) (2005) 237–243.
[28] A. Schönfeld, M. Constantinescu, K. Peters, M. Frenz, Electrospinning of highly concentrated albumin patches by using auxiliary polymers for laser-assisted vascular anastomosis, Biomed. Mater. 13 (5) (2018) 055001.
[29] H. Fong, I. Chun, D.H. Reneker, Beaded nanofibers formed during electrospinning, Polymer 40 (16) (1999) 4585–4592.
[30] J. Panić, M. Vraneš, J. Mirtič, R. Cerc Korošec, Š. Zupančič, S. Gadžurić, J. Kristl, M. Bešter-Rogač, Preparation and characterization of innovative electrospun nanofibers loaded with pharmaceutically applicable ionic liquids, Int. J. Pharm. 615 (2022) 121510.
[31] R. Serôdio, S.L. Schickert, A.R. Costa-Pinto, J.R. Dias, P.L. Granja, F. Yang, A. L. Oliveira, Ultrasound sonication prior to electrospinning tailors silk fibroin/PEO membranes for periodontal regeneration, Mater. Sci. Eng. C 98 (2019) 969–981.
[32] J. Bloustine, T. Virmani, G.M. Thurston, S. Fraden, Light scattering and phase behavior of lysozyme-poly(ethylene glycol) mixtures, Phys. Rev. Lett. 96 (8) (2006) 087803.
[33] A.A. Zaman, B.M. Moudgil, Role of electrostatic repulsion on the viscosity of Bidisperse silica suspensions, J. Colloid Interface Sci. 212 (1) (1999) 167–175.
[34] H. Zhang, S. Xi, Y. Han, L. Liu, B. Dong, Z. Zhang, Q. Chen, W. Min, Q. Huang, Y. Li, J. Liu, Determining electrospun morphology from the properties of protein–polymer solutions, Soft Matter 14 (18) (2018) 3455–3462.
[35] C.J. Angammana, S.H. Jayaram, Analysis of the effects of solution conductivity on electrospinning process and Fiber morphology, IEEE Trans. Ind. Appl. 47 (3) (2011) 1109–1117.
[36] E. Ewaldz, J. Randrup, B. Brettmann, Solvent effects on the elasticity of electrospinnable polymer solutions, ACS Polymers Au 2 (2) (2022) 108–117.
[37] C.E. Brown, Coefficient of variation, in: C.E. Brown (Ed.), Applied Multivariate Statistics in Geohydrology and Related Sciences, Springer, Berlin Heidelberg, Berlin, Heidelberg, 1998, pp. 155–157.
[38] T. Kowalczyk, A. Nowicka, D. Elbaum, T.A. Kowalewski, Electrospinning of bovine serum albumin, optimization and the use for production of biosensors, Biomacromolecules 9 (7) (2008) 2087–2090.
[39] A.A. Al-Shamari, A.M. Abdelghany, H. Alnattar, A.H. Oraby, Structural and optical properties of PEO/CMC polymer blend modified with gold nanoparticles synthesized by laser ablation in water, J. Mater. Res. Technol. 12 (2021) 1597–1605.

[40] C.-Y. Pan, J.-C. Chen, T.-L. Chen, J.-L. Wu, C.-F. Hui, J.-Y. Chen, Piscidin is highly active against Carbapenem-resistant Acinetobacter baumannii and NDM-1-producing Klebsiella pneumonia in a systemic Septicaemia infection mouse model, Mar. Drugs 13 (4) (2015) 2287–2305.
[41] C.M. Valmikinathan, S. Defroda, X. Yu, Polycaprolactone and bovine serum albumin based nanofibers for controlled release of nerve growth factor, Biomacromolecules 10 (5) (2009) 1084–1089.
[42] X. Xu, H. Yu, S. Gao, H.-Q. Mao, K.W. Leong, S. Wang, Polyphosphoester microspheres for sustained release of biologically active nerve growth factor, Biomaterials 23 (17) (2002) 3765–3772.
[43] G. Montalbano, C. Tomasina, S. Fiorilli, S. Camarero-Espinosa, C. Vitale-Brovarone, L. Moroni, Biomimetic scaffolds obtained by electrospinning of collagen-based materials: strategies to hinder the protein denaturation, Materials 14 (16) (2021).
[44] E. Cao, Y. Chen, Z. Cui, P.R. Foster, Effect of freezing and thawing rates on denaturation of proteins in aqueous solutions, Biotechnol. Bioeng. 82 (6) (2003) 684–690.
[45] C. Bs, M. Rr, Enzyme thermostabilization by bovine serum albumin and other proteins: evidence for hydrophobic interactions, Biotechnol. Appl. Biochem. 22 (2) (1995) 203–214.
[46] J.T. Duskey, F. da Ros, I. Ottonelli, B. Zambelli, M.A. Vandelli, G. Tosi, B. Ruozi, Enzyme stability in nanoparticle preparations part 1: bovine serum albumin improves enzyme function, Molecules 25 (20) (2020) 4593.